Chinese Chemical Letters 35 (2024) 109154

Contents lists available at ScienceDirect

Chinese Chemical Letters

journal homepage: www.elsevier.com/locate/cclet

Ultra-highly selective recognition of nucleosides over nucleotides by rational modification of tetralactam macrocycle and its application in enzyme assay

Huan Yao[a,1], Jian Qin[a,1], Yan-Fang Wang[b], Song-Meng Wang[b], Liu-Huan Yi[a], Shi-Yao Li[a], Fangfang Du[a], Liu-Pan Yang[a,*], Li-Li Wang[a,*]

[a] School of Pharmaceutical Science, Postdoctoral Research Station of Basic Medicine, Hengyang Medical School, University of South China, Hengyang 421001, China

[b] Department of Chemistry, Southern University of Science and Technology, Shenzhen 518055, China

ARTICLE INFO

Article history:
Received 29 June 2023
Revised 18 September 2023
Accepted 25 September 2023
Available online 27 September 2023

Keywords:
Rational modification
Biomimetic macrocycle
Ultra-high selectivity
Enzyme assay

ABSTRACT

Artificial macrocycle with high binding selectivity in water is often challenging but urgently needed in various research and application areas. Herein, we report a new water-soluble biomimetic tetralactam macrocycle and realize the ultra-high selectivity to nucleosides over corresponding monophosphate nucleotides by rational modification. The introduction of charged groups at the periphery of *endo*-functionalized cavity makes the selectivity (guanosine to guanosine 5′-monophosphate) increase remarkably from 100 to 1119. Based on the ultra-high selectivity of biomimetic tetralactam macrocycle, the sensitive CD73 enzyme activity assay was then achieved through product-selective fluorescence indicator displacement assay. Furthermore, the capability of the proposed method for inhibitor screening was successfully displayed.

Selective recognition of biomolecules in water is the foundation of numerous biological functions and thus lies at the heart of biochemistry [1–4]. Artificial macrocycle receptors with high selectivity in water is rare but urgently needed in various research and application areas [5–11]. However, it is challenging for artificial macrocycles to achieve high selectivity in water [12–14]. Synthetic hosts generally suffer from low binding selectivity in aqueous environments, particularly for hydrophilic molecules [15–17]. The bioreceptors display excellent selectivity for biomolecules due to their unique structural feature of deep hydrophobic cavity containing polar binding sites. Inspired by the structure of bioreceptors, Jiang group developed a series of *endo*-functionalized naphthotubes and realized the selective recognition of hydrophilic molecules in water recently [18–22]. The inward-directed functional groups endow the corresponding naphthotubes with unique recognition abilities and provide the basis for their applications in sensing, assembly, molecular machines and so on [23–32].

Due to the excellent recognition property of biomimetic naphthotubes, the design concept was further extended to other water-soluble macrocycle with diverse skeleton. A water-soluble tetralactam macrocycle (**H1**) with 2,6-diethoxynaphthalene as sidewalls was reported by Jiang and our group in 2021 [33]. The tetralactam macrocycle has a slightly wider cavity and more hydrogen bond sites than naphthotubes, which makes it more suitable for binding the guests with larger size and more polar sites. For example, the as-synthesized biomimetic tetralactam macrocycle **H1** could recognize riboflavin in water through the synergistic effect of hydrogen bonding and hydrophobic effect, resulting in strong binding ($K_a > 10^7$ L/mol) and thus enhancement of the photostability of riboflavin. Very recently, a novel dual-mode colorimetric and fluorescence indicator displacement assay (IDA) based sensor was constructed using **H1** for urinary uric acid detection [34]. The abundant hydrogen bonding sites and cavity endow the tetralactam macrocycle with excellent selective recognition capacity [35].

These biomimetic hosts possess remarkable recognition properties in water owning to their unique cavity, but the charged tail chain serves mainly to enhance their solubility in water. It is possible to leverage this feature to further improve the binding constants and selectivity. Davis's group revealed that the charged side chains in the bisanthracenyl receptors can indeed be tuned to en-

* Corresponding authors.
E-mail addresses: yanglp@usc.edu.cn (L.-P. Yang), wangll@usc.edu.cn (L.-L. Wang).
[1] These authors contributed equally to this work.

https://doi.org/10.1016/j.cclet.2023.109154
1001-8417/

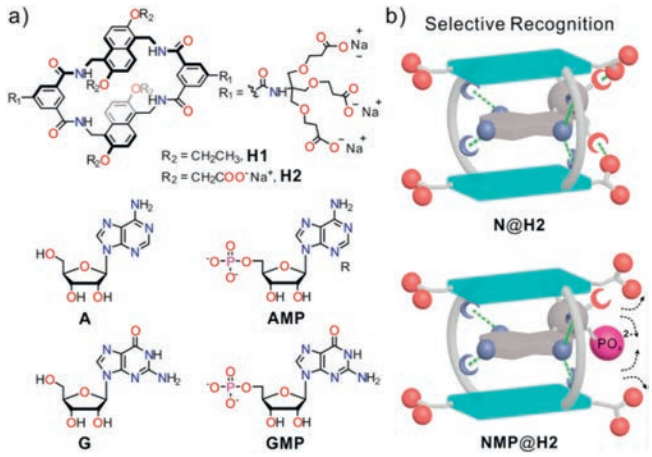

Fig. 1. (a) Chemical structures of tetralactam macrocycle **H1** and **H2**, and relevant nucleotides and nucleosides in this work. (b) Schematic illustration of the highly selective recognition of **H2**.

hance binding properties and adjust selectivity [36]. However, the dendritic side chains located on the benzene group, are a little far away from the entrance of the cavity. We speculate that the binding strength and selectivity should be further increased if the rationally designed groups located near the entrance of the cavity.

For this purpose, the water-soluble tetralactam macrocycle **H1** was reconstructed due to the side chains on the naphthalenes could be easily modified. Four ethyl groups on naphthalenes were replaced by carboxyl groups to obtain macrocycle **H2** (Fig. 1). The introduction of charged chains near the entrance of macrocycle cavity realized the high affinity and ultra-high selectivity (up to 1119) for biomolecule through the synergistic effect of *endo*-functionalized cavity and charged chains. Subsequently, the enzyme assay was performed based on the selective recognition property of **H2**.

As similar to **H1**, the new tetralactam macrocycle **H2** can be readily synthesized from commercial 2,6-dihydroxynaphthalene and 1,3,5-benzenetricarboxylic acid (Scheme S1 in Supporting information). The TFA salt of diamine was synthesized in five simple steps with a total yield of 34% and active ester was obtained following the reported procedure [33]. Amide coupling under a *pseudo*-high-dilution condition was implemented for the cyclization of macrocycle. Then the deprotection procedure was performed to obtain the final water-soluble biomimetic tetralactam host **H2**. The structure of **H2** was confirmed by NMR spectroscopy and high-resolution mass spectrometry (Supporting information). With charged carboxylate groups on the naphthalenes and benzene, the new biomimetic tetralactam host shows good water solubility.

Tetralactam macrocycle has been proven to be an effective receptor for polar aromatic compounds, including biogenic purine and its analogues [37,38]. Nucleosides and nucleotides are important biomolecules and the hydrolysis of nucleotides to nucleosides is a ubiquitous process in organisms [39]. The highly selective recognition of nucleosides and corresponding nucleotides has important scientific significance and broad application prospects. The differences in hydrophilicity and charge for nucleotides and nucleosides may result in the different binding strength to tetralactam macrocycle, which has dendritic negative charged side chain. We speculate that **H2** may display higher selectivity than **H1** due to the additional charged chains near the entrance of the cavity.

The binding ability of **H1** and **H2** to purine nucleosides and corresponding monophosphate nucleotides was first tested by ^{1}H NMR spectra. As shown in Fig. 2 and Figs. S1–S3 (Supporting information), the ^{1}H NMR peaks of host (**H1** and **H2**) and guest (adenosine (**A**) and guanosine (**G**)) all undergo significant shifts after mixing with a 1:1 ratio. In contrast, no obvious or slight shift was observed for corresponding monophosphate, adenosine 5′-monophosphate (**AMP**) and guanosine 5′-monophosphate (**GMP**), demonstrating the much weaker binding affinity of monophosphate nucleotides to tetralactam macrocycles than corresponding purine nucleosides.

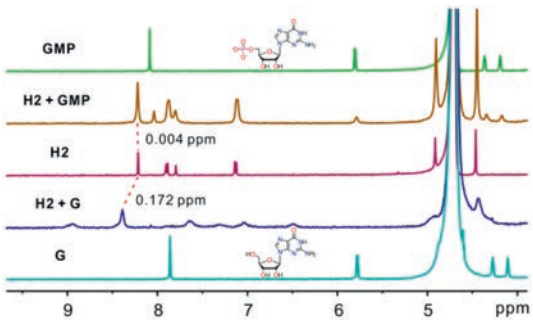

Fig. 2. Partial ^{1}H NMR spectra (500 MHz, D_2O, 0.50 mmol/L, 25 °C) of **GMP**, a 1:1 mixture of **GMP** and **H2**, **H2**, a 1:1 mixture of **G** and **H2**, and **G**.

To quantify the binding constants between hosts and guests and further reveal the driving force, isothermal titration microcalorimetry (ITC) titrations were performed to measure the binding parameters (Figs. S4-S8 in Supporting information). However, the binding constant of three host-guest pairs (**H1**-**AMP**, **H2**-**AMP**, **H2**-**GMP**) could not be determined by ITC titrations due to the low heat release, indicating a weak binding. The binding constants for all eight host-guest pairs were then calculated by UV–vis titration (Figs. S9–S16 in Supporting information). The binding data and calculated selectivity were listed in Table 1. ITC data revealed that enthalpy contributes to the efficient binding while entropy is adverse. This suggests that hydrogen bonding and releasing high-energy water contribute significantly to the binding energy [12,40]. The *n* values are close to 1, suggesting a 1:1 binding stoichiometry ratio. According to the titration results of UV–vis method, the biomimetic hosts **H1** and **H2** all display excellent selectivity to purine nucleosides over corresponding monophosphate nucleotides. The selectivity of **H1** is mainly driven by the difference in guest dehydration energy: nucleotides have a much larger desolvation energy in water than corresponding nucleosides, so binding the more hydrophilic nucleotides has a greater desolvation penalty. Moreover, electrostatic repulsion between the negatively charged dendritic groups of **H1** with nucleotides may also contribute to the selectivity. As expected, the selective factors of **H2** are further enhanced to surpass 800, which are much higher than that of **H1** due to the enhanced charge repulsion effect which bring by the negative groups at the entrance of the cavity. The excellent selectivity of **H2** is comparable to bioreceptor. These results demonstrate that the rational design of biomimetic macrocycle would result in significantly improved binding strength and selectivity.

In order to reveal the better binding affinity and the ultra-high selectivity of purine nucleosides over monophosphate nucleotides, DFT calculations were performed. As shown in Fig. 3a, the guanine base was comfortably encapsulated inside the cavity for **G@H2**. Hydrogen bonds are detected between the carbonyl oxygen atoms of guanine and the NH protons of the hosts, and close contacts suggest that $\pi\cdots\pi$ interactions are also involved in the complex formation. In addition, the carboxyl chain of **H2** formed multiple hydrogen bonds with the ribose and purine base of guanosine, which could explain the slightly enhanced binding constant compared with **H1**. For **GMP@H2** (Fig. 3b), though the host remaining captures the guanine base through multiple hydrogen bonds, the

Table 1
Association constants (K_a, L/mol) and thermodynamic parameters ($\Delta G°$, $\Delta H°$, $-T\Delta S°$, kJ/mol) of **H1** and **H2** with purine nucleosides and corresponding monophosphate nucleotides in water at 25 °C as determined by ITC titration and UV–vis titration.

Host	Guest	ITC				UV	Selectivity
		K_a	$\Delta G°$	$\Delta H°$	$-T\Delta S°$	K_a	
H1	**A**	6.8×10^3	−21.9	−31.6	9.7	6.2×10^3	203
	AMP	–	–	–	–	25.6	
	G	1.8×10^5	−30.0	−49.2	19.2	2.4×10^5	100
	GMP	2.5×10^3	−19.4	−42.6	23.2	2.4×10^3	
H2	**A**	6.4×10^3	−21.7	−32.5	10.7	5.3×10^3	707
	AMP	–	–	–	–	7.5	
	G	3.3×10^5	−31.5	−52.1	20.7	4.7×10^5	1119
	GMP	–	–	–	–	4.0×10^2	

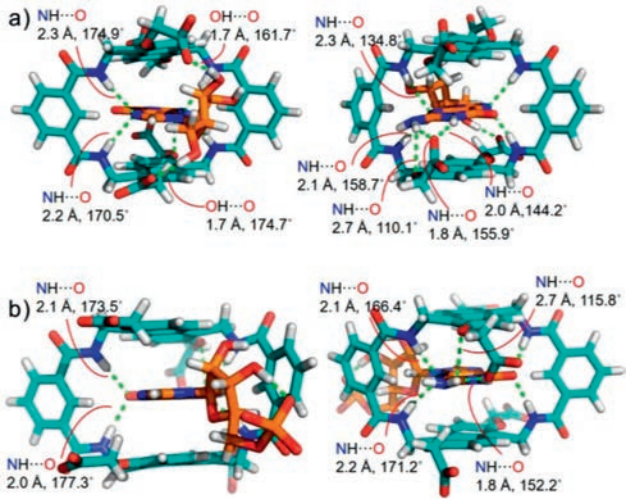

Fig. 3. Energy-minimized structures of (a) **G@H2** and (b) **GMP@H2** obtained by DFT (ωB97XD/6–31G(d,p)) calculations with the SMD solution model in water.

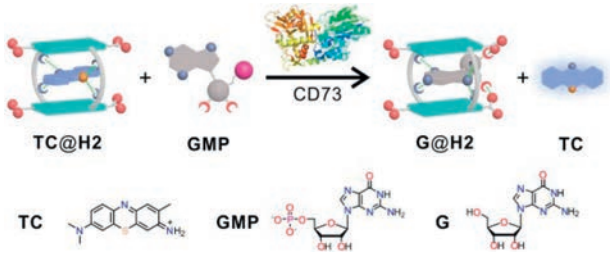

Fig. 4. Schematic illustration of CD73 activity monitoring with a switch-on fluorescence response by **TC@H2** reporter pair.

strong electrostatic repulsion between the phosphoric acid group of **GMP** with the carboxyl chains of **H2** would decrease the stability of the complex. For **G**/**GMP** with tetralactam macrocycle **H1**, the noncovalent interaction force in cavity was similar to that of **H2**, but no additional interaction was seen between the ethyl groups and guests (Figs. S17 and S18 in Supporting information). The synergistic effect of large desolvation penalty and enhanced charge repulsion effect result in a much lower binding constant for monophosphate nucleotides with **H2**.

Dephosphorylation is an important process in controlling a wide range of biological activities [41]. The dephosphorylation of nucleotides was controlled by ecto-5′-nucleotidase (CD73), a membrane-bound enzyme which could hydrolyze nucleoside-5-monophosphates yielding the respective nucleoside and phosphate [42,43]. CD73 is also one of the emerging targets for cancer immunotherapy and serves as a crucial metabolic and immune checkpoint [44,45]. Elevated CD73 levels in the tumor tissue are linked to poor patient survival. Therefore, the development of a simple, rapid and sensitive method to evaluate the enzymatic activity of CD73 is urgently required [46].

Based on the ultra-high selective recognition capacity of macrocycle **H2**, the substrate-selective indicator displacement assay (IDA) strategy could be exploited for CD73 enzyme activity assay [47–49]. To develop the supramolecular tandem assays for the enzyme function of CD73 based on **H2**, a suitable fluorescent dye must be selected as the signal report unit. According to our previous report, phenoxazine dyes were ideal indicators to construct IDA sensors with tetralactam macrocycle due to their obvious change of fluorescence intensity in and out of the cavity and moderate binding constant. In this research, toloniumchloride (**TC**) dye was selected as the fluorescence indicator for enzyme activity assay. The constructed IDA for CD73 could be demonstrated as a product-selective assay (Fig. 4). **TC** dye formed a strong inclusion complex with **H2**, which showed much weaker fluorescence intensity compared with free **TC**. Moreover, the substrate **GMP** had a low affinity to **H2** and caused negligible interference with the **TC@H2** complex. The CD73 enzyme could hydrolyze the phosphoester bond of **GMP** and generate **G** product, a much stronger competitor which displaced **TC** from the macrocycle and resulted in a fluorescence recovery. The CD73 activity could be monitored by the switch-on fluorescence response of **TC**.

The fluorescence intensity of **TC** decreases gradually with the addition of **H2**. The K_a was determined as 4.2×10^5 L/mol (Fig. S19 in Supporting information) by the nonlinear fitting of fluorescence titration. At the same time, the K_a was also calculated by UV–vis titration and gave a value of 6.3×10^5 L/mol (Fig. S20 in Supporting information), which was comparable to **G** with **H2**. To construct the sensitive fluorescence IDA sensor, the concentration of **TC** and **H2** were set to 1 and 9 μmol/L, respectively, which was shown to be significant signal change and highly sensitive according to our previous research [34]. The optical responses of the **TC@H2** complexes to **G** and **GMP** were further studied. The fluorescence of **TC** shows obvious recovery with the addition of **G** while keeping invariable with the addition of **GMP** in water at 25 °C (Fig. S21 and S22 in Supporting information). As a control experiment, the fluorescence titrations of **H2** alone with guest **G** and **GMP** were performed. No obvious fluorescence was observed for **H2** alone and keeping invariable with the gradual addition of guest (Fig. S23 in Supporting information).

Though the elevated temperature and buffer solution result in the decreased binding strength to 3.3×10^5 L/mol between **H2** and guest (Fig. S24 in Supporting information), the **TC@H2** pair still displays remarkable differentiated fluorescence response, which makes the possibility to construct the IDA sensing system for CD73 activity (Fig. S25 in Supporting information). Prior to the enzyme

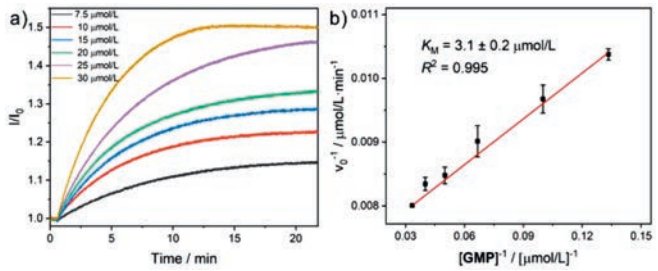

Fig. 5. (a) Determination of the K_M value by monitoring CD73 (0.3 μg/mL) activity with various concentrations of **GMP** (7.5–30 μmol/L) in the presence of **TC@H2** reporter pair (1/9 μmol/L, $\lambda_{ex} = 610$ nm, $\lambda_{em} = 660$ nm). The experiments were performed in Tris–HCl buffer (25 mmol/L, pH 7.4) containing 0.25 mmol/L $MgCl_2$ (activator of CD73 activity) at 37 °C. (b) The Lineweaver-Burk plot for CD73.

assay, the effect of **H2** on the activity of CD73 was also investigated. As CD73 can catalyze the degradation of **GMP** into free inorganic phosphate, the CD73 enzymatic activity could be monitored by assaying the concentration of inorganic phosphate based on the Malachite green phosphate assay [50]. The results show that the macrocycle **H2** has no obvious effect on the absorption intensity at 620 nm, which is correlated with the concentration of free inorganic phosphate (Fig. S26 in Supporting information). There was no obvious effect of **H2** on the activity of CD73.

In fact, the CD73 assay worked as designed and showed the expected response of the fluorescence on the activity of the enzyme with fixed **GMP** concentration (Fig. S27 in Supporting information). For the measurement of enzyme kinetic parameters, a range of substrate concentrations was used to monitor the enzyme kinetics (Fig. 5a). According to the Michaelis-Menten model, the data was fitted and gave a K_M value of 3.1 ± 0.2 μmol/L (Fig. 5b), which was in agreement with the literature value [46].

After successfully verifying the effectiveness of **TC@H2** as a sensor for detecting CD73 activity, we further evaluated its potential as a screening tool for enzyme inhibitors, a crucial aspect of drug candidate assessment. Adenosine diphosphate (**ADP**) and adenosine triphosphate (**ATP**), two different types of CD73 inhibitors were selected as samples to investigate the screening ability of IDA sensing system. **ADP** and **ATP** showed negligible effect to the fluorescence of **TC** dye and **TC@H2** reporter pair (Figs. S28 and S29 in Supporting information), demonstrating the weak binding of inhibitors with **H2**. These compounds caused an obvious inhibition of CD73 activity, and a decrease of CD73 activity was displayed with the gradual increasing concentrations of **ADP** and **ATP**, which could be observed in a sharp decrease in the initial conversion rates of **GMP** (Fig. 6 and Fig. S30 in Supporting information). The IC_{50} of

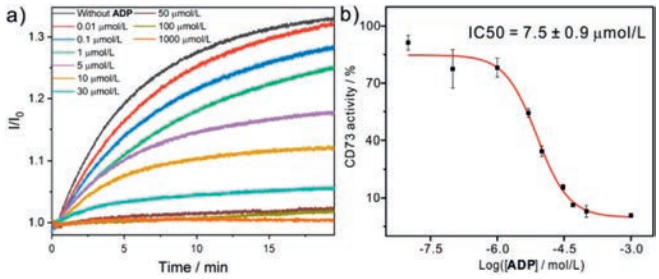

Fig. 6. (a) Continuous fluorescent assay for CD73 activity inhibition by **ADP** (0.01–1000 μmol/L) with the **TC@H2** reporter pair (1/9 μmol/L, $\lambda_{ex} = 610$ nm, $\lambda_{em} = 660$ nm), CD73 (0.3 μg/mL) and **GMP** (20 μmol/L). (b) Dose-response curve and associated plot analysis for CD73 activity inhibition by **ADP**. The experiments were performed in Tris–HCl buffer (25 mmol/L, pH 7.4) containing 0.25 mmol/L $MgCl_2$ (activator of CD73 activity) at 37 °C.

ADP and **ATP** against CD73 was calculated to be 7.5 ± 0.9 μmol/L and 3.6 ± 0.5 μmol/L, respectively.

In summary, we reported a new biomimetic tetralactam macrocycle (**H2**) with high binding selectivity through the synergetic effect of *endo*-functionalized cavity and enhanced charge repulsion effect. The selectivity of **H2** to nucleoside and corresponding nucleotide is up to 1119, which is much higher than **H1**, and is comparable to bioreceptor. The charged chains at the entrance of the cavity are responsible for the improved selectivity. This research provides an example of the rational design of macrocycle to enhance binding selectivity in water. Furthermore, a fluorescence IDA-based sensing assay for enzyme activity detection was successfully constructed based on **H2** and **TC** dye. The ability of this method for enzyme inhibitors screening was also displayed. We anticipate that this design strategy will stimulate the development of other synthetic receptors featuring outstanding properties.

Declaration of competing interest

The authors declare that they have no known competing financial interests or personal relationships that could have appeared to influence the work reported in this paper.

Acknowledgments

This research was financially supported by National Natural Science Foundation of China (Nos. 22174059 and 22201128), Hunan Provincial Natural Science Foundation of China (Nos. 2022JJ40363, 2022JJ40365 and 2022RC1230), the Excellent youth funding of Hunan Provincial Education Department (No. 22B0460), and China Postdoctoral Science Foundation (No. 2022M721542).

Supplementary materials

Supplementary material associated with this article can be found, in the online version, at doi:10.1016/j.cclet.2023.109154.

References

[1] L. Escobar, P. Ballester, Chem. Rev. 121 (2021) 2445–2514.
[2] P.C. Weber, D.H. Ohlendorf, J.J. Wendoloski, et al., Science 243 (1989) 85–88.
[3] W. Liu, S.K. Samanta, B.D. Smith, et al., Chem. Soc. Rev. 46 (2017) 2391–2403.
[4] J. Wang, L. Zhou, J. Bei, et al., J. Colloid Interface Sci. 620 (2022) 187–198.
[5] B.D. Smith, Synthetic Receptors for Biomolecules, Royal Society of Chemistry, London, UK, 2015.
[6] H.J. Schneider, A.K. Yatsimirsky, Chem. Soc. Rev. 37 (2008) 263–277.
[7] L. Catti, R. Sumida, M. Yoshizawa, Coord. Chem. Rev. 460 (2022) 214460.
[8] S.L. Li, T. Xiao, C. Lin, et al., Chem. Soc. Rev. 41 (2012) 5950–5968.
[9] Y.L. Ma, S. Yan, X.J. Xu, et al., Chin. Chem. Lett. 35 (2024) 108645.
[10] J. Wang, M. Cen, J. Wang, et al., Chin. Chem. Lett. 33 (2022) 1475–1478.
[11] J. Wang, J. Bei, X. Guo, et al., Biosens. Bioelectron. 208 (2022) 114220.
[12] H. Yao, H. Ke, X. Zhang, et al., J. Am. Chem. Soc. 140 (2018) 13466–13477.
[13] K. Yazaki, Y. Sei, M. Akita, et al., Nat. Commun. 5 (2014) 5179.
[14] W. Liu, A. Johnson, B.D. Smith, J. Am. Chem. Soc. 140 (2018) 3361–3370.
[15] L.P. Yang, X. Wang, H. Yao, et al., Acc. Chem. Res. 53 (2020) 198–208.
[16] E. Persch, O. Dumele, F. Diederich, Angew. Chem. Int. Ed. 54 (2015) 3290–3327.
[17] C.D. Zhao, H. Yao, S.Y. Li, et al., Chin. Chem. Lett. 35 (2024) 108879.
[18] G.B. Huang, S.H. Wang, H. Ke, et al., J. Am. Chem. Soc. 138 (2016) 14550–14553.
[19] L.L. Wang, Z. Chen, W.E. Liu, et al., J. Am. Chem. Soc. 139 (2017) 8436–8439.
[20] X. Huang, X. Wang, M. Quan, et al., Angew. Chem. Int. Ed. 60 (2021) 1929–1935.
[21] X. Wang, M. Quan, H. Yao, et al., Nat. Commun. 13 (2022) 2291.
[22] H. Zhou, X.Y. Pang, X. Wang, et al., Angew. Chem. Int. Ed. 60 (2021) 25981–25987.
[23] L.L. Wang, M. Quan, T.L. Yang, et al., Angew. Chem. Int. Ed. 59 (2020) 23817–23824.
[24] H. Ke, L.P. Yang, M. Xie, et al., Nat. Chem. 11 (2019) 470–477.
[25] Z. Chen, M. Quan, Y.W. Dong, et al., Chem. Commun. 58 (2022) 9413–9416.
[26] L.M. Bai, H. Zhou, W.E. Liu, et al., Chem. Commun. 55 (2019) 3128–3131.
[27] W.E. Liu, Z. Chen, L.P. Yang, et al., Chem. Commun. 55 (2019) 9797–9800.
[28] L.S. Zheng, J.S. Cui, W. Jiang, Angew. Chem. Int. Ed. 58 (2019) 15136–15141.
[29] W. Liu, L. Kong, M. Quan, et al., Chin. Chem. Lett. 33 (2022) 4896–4899.
[30] Q. Shi, L. Cao, Y. Chen, et al., Chin. Chem. Lett. 34 (2023) 108138.
[31] L.P. Yang, H. Ke, H. Yao, et al., Angew. Chem. Int. Ed. 60 (2021) 21404–21411.
[32] Y.L. Ma, C. Sun, Z. Li, et al., CCS Chem. 4 (2022) 1977–1989.

[33] H. Zhang, L.L. Wang, X.Y. Pang, et al., Chem. Commun. 57 (2021) 13724–13727.
[34] H. Yao, S.Y. Li, H. Zhang, et al., Chem. Commun. 59 (2023) 5411–5414.
[35] S.Y. Li, H. Yao, H. Hu, et al., Chem. Commun. 59 (2023) 7204–7207.
[36] H. Destecroix, C.M. Renney, T.J. Mooibroek, et al., Angew. Chem. Int. Ed. 54 (2015) 2057–2061.
[37] D. Van Eker, S.K. Samanta, A.P. Davis, Chem. Commun. 56 (2020) 9268–9271.
[38] A.P. Davis, Chem. Soc. Rev. 49 (2020) 2531–2545.
[39] F. Di Virgilio, E. Adinolfi, Oncogene 36 (2017) 293–303.
[40] F. Biedermann, W.M. Nau, H.J. Schneider, Angew. Chem. Int. Ed. 53 (2014) 11158–11171.
[41] F. Ardito, M. Giuliani, D. Perrone, et al., Int. J. Mol. Med. 40 (2017) 271–280.
[42] H. Castrop, Y. Huang, S. Hashimoto, et al., J. Clin. Invest. 114 (2004) 634–642.
[43] M.V. Sorensen, S. Grossmann, M. Roesinger, et al., Kidney Int. 83 (2013) 811–824.
[44] J. Stagg, U. Divisekera, N. McLaughlin, et al., Proc. Natl. Acad. Sci. U. S. A. 107 (2010) 1547–1552.
[45] B. Allard, S. Pommey, M.J. Smyth, et al., Clin. Cancer Res. 19 (2013) 5626–5635.
[46] M. Freundlieb, H. Zimmermann, C.E. Muller, Anal. Biochem. 446 (2014) 53–58.
[47] W.M. Nau, G. Ghale, A. Hennig, et al., J. Am. Chem. Soc. 131 (2009) 11558–11570.
[48] Z. Zheng, S. Ren, W.C. Geng, et al., Chem. Asian J. 17 (2022) e202200106.
[49] D.S. Guo, J. Yang, Y. Liu, Chem. Eur. J. 19 (2013) 8755–8759.
[50] B. Allard, I. Cousineau, K. Spring, et al., Methods Enzymol. 629 (2019) 269–289.